



# Phase structures and transitions of Born–Infeld black holes in a grand canonical ensemble

Kangkai Liang<sup>a</sup>, Peng Wang<sup>b</sup>, Houwen Wu<sup>c</sup>, Mingtao Yang<sup>d</sup>

Center for Theoretical Physics, College of Physical Science and Technology, Sichuan University, Chengdu 610064, China

Received: 10 December 2019 / Accepted: 17 February 2020 / Published online: 29 February 2020  
© The Author(s) 2020

**Abstract** To make a Born–Infeld (BI) black hole thermally stable, we consider two types of boundary conditions, i.e., the asymptotically anti-de Sitter (AdS) space and a Dirichlet wall placed in the asymptotically flat space. The phase structures and transitions of these two types of BI black holes, namely BI-AdS black holes and BI black holes in a cavity, are investigated in a grand canonical ensemble, where the temperature and the potential are fixed. For BI-AdS black holes, the globally stable phases can be the thermal AdS space. For small values of the potential, there is a Hawking–Page-like first order phase transition between the BI-AdS black holes and the thermal-AdS space. However, the phase transition becomes zeroth order when the values of the potential are large enough. For BI black holes in a cavity, the globally stable phases can be a naked singularity or an extremal black hole with the horizon merging with the wall, which both are on the boundaries of the physical parameter region. The thermal flat space is never globally preferred. Besides a first order phase transition, there is a second order phase transition between the globally stable phases. Thus, it shows that the phase structures and transitions of BI black holes with these two different boundary conditions have several dissimilarities.

## 1 Introduction

The study of black hole thermodynamics has continued to fascinate researchers since the pioneering work [1–3], where Hawking and Bekenstein found that black holes possess the temperature and the entropy. However, it is well known that a Schwarzschild black hole in asymptotically flat space is thermally unstable because of its negative specific heat. To study black hole thermodynamics in a thermally stable system, one can impose appropriate boundary conditions. For example, putting black holes in the anti-de Sitter (AdS) space can make them thermally stable since the AdS boundary acts as a reflecting wall for the Hawking radiation. The investigations of the thermodynamic properties of AdS black holes have come a long way since the discovery of the Hawking–Page phase transition [4], i.e., a phase transition between the thermal AdS space and the Schwarzschild-AdS black hole. Later, with the advent of the AdS/CFT correspondence [5–7], there has been much interest in studying the phase transitions of AdS black holes [8–13]. From the holographic perspective, we are eager to find out whether the duality is independent of the details of the boundary conditions of the bulk space-time. It is therefore interesting to study the thermodynamics and phase structures of black holes under different boundary conditions and look for similarities or dissimilarities to the AdS case.

On the other hand, placing a Schwarzschild black hole in a cavity in the asymptotically flat space, York showed that the black hole can be thermally stable and has similar phase structure and transition to these of a Schwarzschild-AdS black hole [14]. Specifically, the Schwarzschild black hole in a cavity undergoes a Hawking–Page-like transition to the thermal flat space as the temperature decreases. The thermodynamics and phase structure of a Reissner–Nordstrom (RN) black hole in a cavity have been studied in a grand canonical ensemble [15] and a canonical ensemble [16, 17], which showed that the phase structures of the RN black

## Contents

1 Introduction	1
2 Born–Infeld AdS black holes	2
3 Born–Infeld black holes in a cavity	5
4 Discussion and conclusion	10
References	12

<sup>a</sup> e-mail: 2016141221063@stu.scu.edu.cn

<sup>b</sup> e-mail: pengw@scu.edu.cn

<sup>c</sup> e-mail: iverwu@scu.edu.cn (corresponding author)

<sup>d</sup> e-mail: 2017141221040@stu.scu.edu.cn

hole in a cavity and the RN-AdS black hole have extensive similarities. In a series of paper [18–23], the phase structures of various black brane systems in a cavity were investigated in a grand canonical ensemble and a canonical ensemble, and it was found that Hawking-Page-like or van der Waals-like phase transitions always occur except for some special cases. In [24–27], boson stars and hairy black holes in a cavity were considered, and it showed that the phase structure of the gravity system in a cavity is strikingly similar to that of holographic superconductors in the AdS gravity. The stabilities of solitons, stars and black holes in a cavity were also studied in [28–35], which showed that the nonlinear dynamical evolution of a charged black hole in a cavity could end in a quasi-local hairy black hole. The thermodynamic behavior of de Sitter black holes in a cavity has been discussed in the extended phase space [36]. Recently, McGough et al. [37] proposed that the holographic dual of  $T\bar{T}$  deformed  $CFT_2$  is a finite region of  $AdS_3$  with the wall at finite radial distance, which further motivates us to explore the properties of a black hole in a cavity.

The Born–Infeld (BI) electrodynamics is a particular example of a nonlinear electrodynamics, which is an effective model incorporating quantum corrections to Maxwell electromagnetic theory. BI electrodynamics was first proposed to smooth divergences of the electrostatic self-energy of point charges by introducing a cutoff on electric fields [38]. Later, it is realized that BI electrodynamics can emerge from the low energy limit of string theory, which encodes the low-energy dynamics of D-branes. Coupling the BI electrodynamics field to gravity, the BI black hole solution was first obtained in [39,40]. For the BI black holes in asymptotically AdS space, the thermodynamic behavior and phase transitions have been investigated in [41–62]. Specifically, the phase structures and transitions of 4D BI-AdS black holes in a canonical ensemble were studied in [47,55,58], which showed that a reentrant phase transition was always observed in a certain region of the parameter space. Meanwhile, the thermodynamics and phase transitions in a grand canonical ensemble have been analyzed in [42], which showed that the system undergoes the first and zeroth order phase transitions between the black hole solutions and the thermal AdS space. On the other hand, by placing a BI black hole in a spherical thermal cavity, we recently discussed the phase structures and transitions of the canonical ensemble of this system [63], which were found to have dissimilarities from these of the BI-AdS black holes.

In this paper, we study the phase structures and transitions of the grand canonical ensemble of BI black holes using both asymptotically AdS and the Dirichlet wall boundary conditions. So the gauge potential is fixed rather than the charge on the boundaries in this paper. In the framework of the AdS/CFT duality, the grand canonical ensemble is more

relevant than the canonical ensemble. Although the phase structures and transitions of BI-AdS black holes in the grand ensemble have already been investigated in [42], we carry out the analysis in a more thorough way with a broader survey of the parameter space. The phase diagrams in the parameter space are obtained, which can be used to make a comparison with these of BI black holes in a cavity. In the second part of this paper, we analyze the phase structures and transitions of BI black hole in a cavity in the grand canonical ensemble. We find that the thermal flat space, which is the counterpart of the thermal AdS space in the BI-AdS case, can never be the globally stable phase. Moreover, the system has no zeroth order transition, but instead a second order transition occurs. It turns out that the results of the BI black holes in a cavity and BI-AdS black holes have several dissimilarities.

The rest of this paper is organized as follows. In Sect. 2, we study the phase structures and transitions of BI-AdS black holes and give the phase diagrams, e.g., Figs. 2 and 4. In Sect. 3, we discuss the phase structures and transitions of BI black holes in a cavity. The related phase diagrams are given in Figs. 7 and 10, from which one can read the phase structures and transitions. Section 4 is devoted to our discussion and conclusion.

## 2 Born–Infeld AdS black holes

In this section, we consider the phase structures and transitions of BI-AdS black holes in a grand canonical ensemble. The action of a  $(3 + 1)$  dimensional model of gravity coupled to a Born–Infeld electromagnetic field  $A_\mu$  is

$$S = \int d^4x \sqrt{-g} [R - 2\Lambda + \mathcal{L}_{BI}(F)], \quad (1)$$

where the cosmological constant  $\Lambda = -3/l^2$ , and we take  $16\pi G = 1$  for simplicity. The Born–Infeld electrodynamics Lagrangian density is

$$\mathcal{L}_{BI}(F) = -\frac{1}{a} \left( 1 - \sqrt{1 - a F^{\mu\nu} F_{\mu\nu}/2} \right),$$

where  $F_{\mu\nu} = \partial_\mu A_\nu - \partial_\nu A_\mu$ , and the Born–Infeld parameter  $a$  is related to the string tension  $\alpha'$  as  $a = (2\pi\alpha')^2 > 0$ . When  $a \rightarrow 0$ ,  $\mathcal{L}_{BI}(F)$  reduces to the Lagrangian of the Maxwell field. The Born–Infeld AdS black hole solution was obtained in [39,40]:

$$ds^2 = -f(r) dt^2 + \frac{dr^2}{f(r)} + r^2 (d\theta^2 + \sin^2\theta d\phi^2),$$

$$A = A_t(r) dt. \quad (2)$$

where

$$f(r) = 1 - \frac{M}{8\pi r} + \frac{r^2}{l^2} - \frac{Q^2}{6\sqrt{r^4 + aQ^2} + 6r^2} + \frac{Q^2}{3r^2} {}_2F_1\left(\frac{1}{4}, \frac{1}{2}, \frac{5}{4}; -\frac{aQ^2}{r^4}\right),$$

$$A'_t(r) = \frac{Q}{\sqrt{r^4 + aQ^2}}. \tag{3}$$

Here  $M$  and  $Q$  are the mass and the charge of the black hole, respectively, and  ${}_2F_1(a, b, c; x)$  is the hypergeometric function.

At the horizon  $r = r_+$ , one has that  $f(r_+) = 0$ , and the Hawking temperature is given by

$$T = \frac{f'(r_+)}{4\pi} = \frac{1}{4\pi r_+} \left( 1 - \frac{1}{2} \frac{Q^2}{r_+^2 + \sqrt{r_+^4 + aQ^2}} \right). \tag{4}$$

Requiring  $A_t(r)$  at the horizon to be zero, it can show that the gauge potential measured with respect to the horizon is

$$\Phi = 4\pi A_t(\infty) = \frac{4\pi Q}{r_+} {}_2F_1\left(\frac{1}{4}, \frac{1}{2}, \frac{5}{4}; -\frac{aQ^2}{r_+^4}\right). \tag{5}$$

In the limit of  $r_+ \rightarrow +\infty$ , BI-AdS black holes would reduce to RN-AdS black holes, and we find that

$$\Phi(r_+, Q, a) \sim \frac{4\pi Q}{r_+} \text{ and } T \sim \frac{3r_+}{4\pi l^2}. \tag{6}$$

As  $r_+ \rightarrow 0$ , Eqs. (4) and (5) gives

$$\Phi \sim \sqrt{\frac{Q}{2\sqrt{a}}} \Phi_c \text{ and } T \sim \frac{1}{4\pi r_+} \left( 1 - \frac{\Phi^2}{\Phi_c^2} \right), \tag{7}$$

where  $\Phi_c \equiv 4\sqrt{2\pi} \Gamma\left(\frac{1}{4}\right) \Gamma\left(\frac{5}{4}\right) \sim 32.95$ . So when  $\Phi > \Phi_c$ ,  $T \rightarrow -\infty$  as  $r_+ \rightarrow 0$ , which means that  $r_+$  has a nonzero minimum value. On the other hand,  $T \rightarrow +\infty$  as  $r_+ \rightarrow 0$  for  $\Phi < \Phi_c$ , and hence  $r_+$  can go to zero in this case.

To study the phase structures and transitions, we need to consider the free energy of the black hole. The free energy of a BI-AdS black hole in a canonical ensemble was obtained by computing the Euclidean action in [58], where an extra boundary term  $S_{\text{surf}}$  was introduced to keep the charge fixed instead of the potential. However for the grand canonical ensemble,  $S_{\text{surf}}$  is not needed any more. Excluding the contribution of  $S_{\text{surf}}$ , the computation of the Euclidean action in [58] then gives the free energy of the BI-AdS black hole in the grand canonical ensemble:

$$F = M - TS - Q\Phi, \tag{8}$$

where  $S = 16\pi^2 r_+^2$  is the entropy of the black hole. For the later convenience, we can express quantities in units of  $l$ :

$$\tilde{T} = Tl, \tilde{r}_+ = r_+/l, \tilde{Q} = Q/l, \tilde{a} = al^{-2} \text{ and } \tilde{F} \equiv F/l. \tag{9}$$

Note that the potential  $\Phi$  is dimensionless.

To find the phase structures of the black hole, one needs to use Eqs. (4) and (5) to express the horizon radius  $\tilde{r}_+$  in terms of the temperature  $\tilde{T}$  and the potential  $\Phi$ :  $\tilde{r}_+ = \tilde{r}_+(\tilde{T}, \Phi)$ . When  $\Phi < \Phi_c$ ,  $T \rightarrow +\infty$  in the limits of  $r_+ \rightarrow 0$  and  $r_+ \rightarrow +\infty$ , which implies that  $\tilde{r}_+(\tilde{T}, \Phi)$  are multivalued. In the left panel of Fig. 1, we plot  $\tilde{T}$  as a function of  $\tilde{r}_+$  and  $\Phi$  with  $\tilde{a} = 0.1$ . We plot  $\tilde{r}_+$  against  $\tilde{T}$  for various values of  $\Phi$  with  $\tilde{a} = 0.1$  in the right panel of Fig. 1. When  $\Phi = 10, 25$  and  $32$ , there are two family of black holes of different sizes with the same values of  $\tilde{T}$  and  $\Phi$ : Small BH and Large BH. When  $\Phi = 35 > \Phi_c$ , there is only one branch: BH. To consider the thermodynamic stabilities against thermal fluctuations, we consider the specific heat at constant potential:

$$C_\Phi = T \left( \frac{\partial S}{\partial T} \right)_\Phi = 32l^2 \pi^2 \tilde{r}_+ \tilde{T} \frac{\partial \tilde{r}_+(\tilde{T}, \Phi)}{\partial \tilde{T}}. \tag{10}$$

The thermal stable black holes have  $C_\Phi \geq 0$ , which means  $\partial \tilde{r}_+ / \partial \tilde{T} > 0$ . So the BH/large BH branches in Fig. 1 are thermally stable. To discuss the phase transitions of the black hole, we need to calculate the free energies of different branches and compare them. Moreover, the thermal AdS space with a constant gauge potential is also a classical solution of the action (1). Therefore, the thermal AdS space is also considered for the phase transitions in the grand canonical ensemble.

We find that there are four regions in the  $\tilde{a}$ - $\Phi$  phase space of the BI-AdS black holes, in each of which the black holes have different behavior of the branches of  $\tilde{r}_+(\tilde{T}, \Phi)$  and phase structure. These four regions of the  $\tilde{a}$ - $\Phi$  phase space are mapped in Fig. 2. In what follows, we discuss the phase structures and transitions in the four regions:

- Region I: The temperature of a BI-AdS black hole in this region has a positive minimum value  $\tilde{T}_{\text{min}}$ . For  $\tilde{T} \geq \tilde{T}_{\text{min}}$ , there are two branches of black holes: small BH and large BH. The free energies of the two branches with  $\tilde{a} = 0.1$  and  $\Phi = 10$  and the thermal AdS space are plotted in Fig. 3a. The large BH branch always has lower free energy than the small BH branch. The thermal AdS space is the only phase when  $\tilde{T} < \tilde{T}_{\text{min}}$ . At  $\tilde{T}_{\text{min}}$ , the black hole appears, and its free energy is larger than that of the thermal AdS space. As  $\tilde{T}$  increases from  $\tilde{T}_{\text{min}}$ , the free energy of large BH decreases while that of the thermal AdS space is constant. They cross each other at some

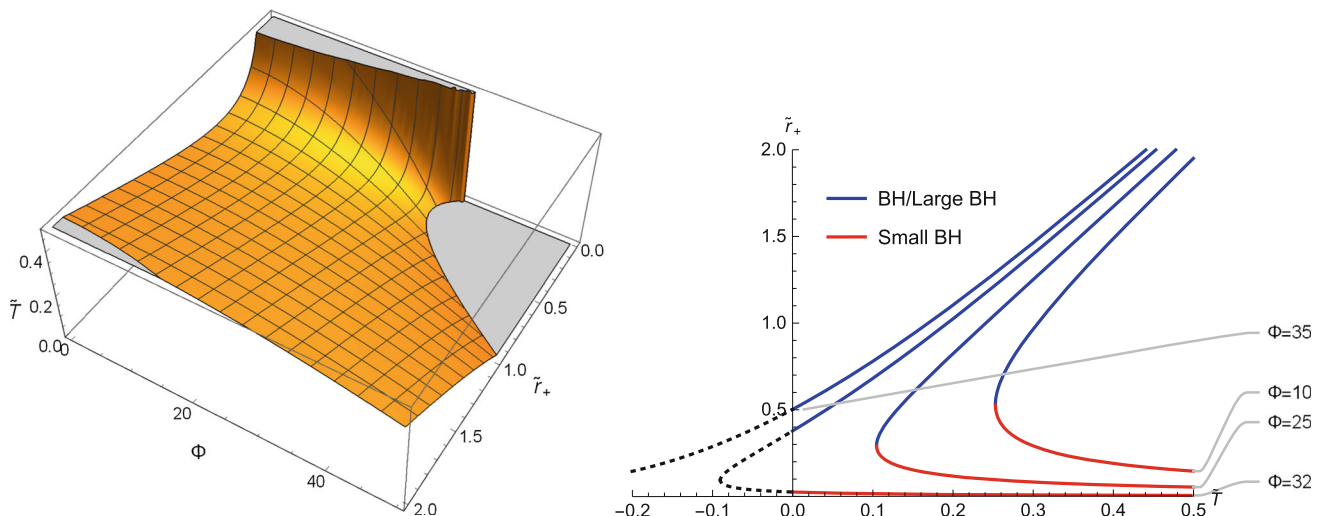


**Fig. 1** Plots of  $\tilde{T}(\tilde{r}_+, \Phi)$  and  $\tilde{r}_+(\tilde{T}, \Phi)$  for BI-AdS black holes with  $\tilde{a} = 0.1$ . Left panel: plot of  $\tilde{T}$  as a function of  $\tilde{r}_+$  and  $\Phi$ .  $\tilde{T}$  is negative in the gray area. Right panel: plot of  $\tilde{r}_+$  against  $\tilde{T}$  for various values of  $\Phi$ . Since thermally stable phases have  $\partial\tilde{r}_+/\partial\tilde{T} > 0$ , the BI-AdS black holes on blue/red branches of the  $\tilde{r}_+(\tilde{T}, \Phi)$  curves are thermally

stable/unstable. We denote the blue branches by Large BH (or BH if there is only one branch) and red branches by Small BH. The black holes on the black dashed branches have negative temperature, which are unphysical

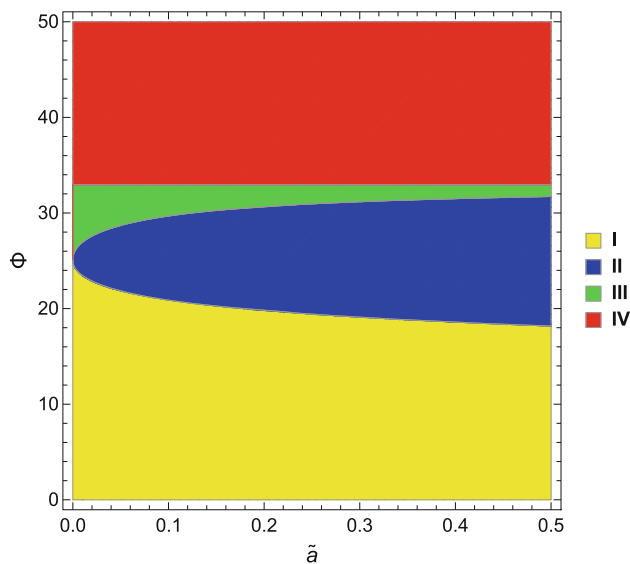


**Fig. 2** The four regions in the  $\tilde{a} - \Phi$  phase space of BI-AdS black holes, each of which possesses distinct behavior of the phase structures and transitions. Varying the temperature, a first order LBH/thermal AdS phase transition occurs in Regions I while a zeroth order LBH/thermal AdS phase transition occurs in Regions II. There are no phase transitions in Regions III and IV

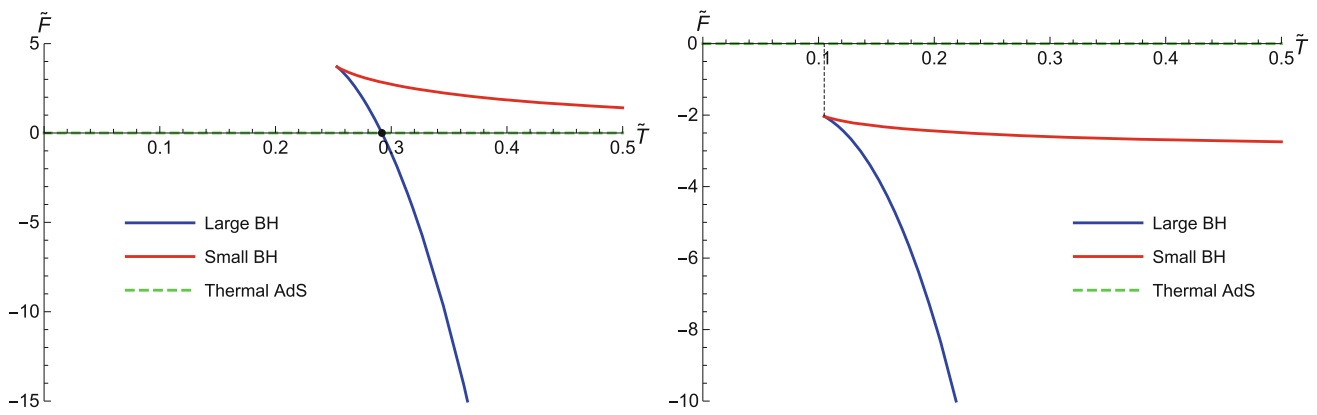
point, where a first-order transition occurs, and large BH then becomes globally stable.

- Region II: As in Region I, only the thermal AdS space exists for  $\tilde{T} < \tilde{T}_{\min}$ , and the BI-AdS black hole appears and has two branches for  $\tilde{T} > \tilde{T}_{\min}$ . The free energies of the two branches with  $\tilde{a} = 0.1$  and  $\Phi = 25$  and the

thermal AdS space are plotted in Fig. 3b. However, at  $\tilde{T} = \tilde{T}_{\min}$ , the free energy of the black hole is smaller than that of the thermal AdS space. So there is a finite jump in the free energy at  $\tilde{T} = \tilde{T}_{\min}$  leading to a zeroth order phase transition from the thermal AdS space to large BH.

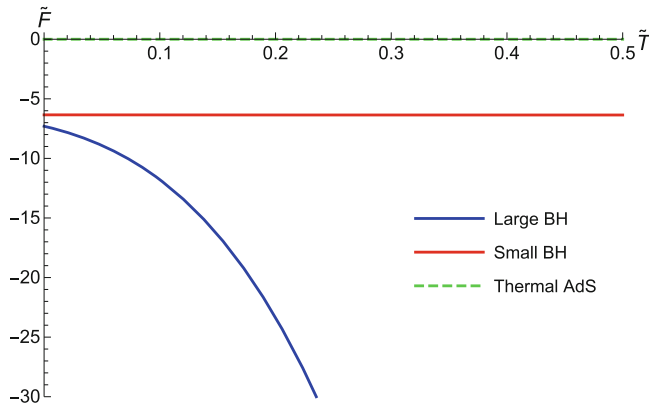
- Region III: In this region, the BI-AdS black holes can exist for all non-negative values of  $\tilde{T}$ , which have large BH and small BH branches. The free energies of the two branches with  $\tilde{a} = 0.1$  and  $\Phi = 32$  and the thermal AdS space are plotted in Fig. 3c. It shows that large BH always has the smallest free energy. So there is no phase transition, and the global stable phase is large BH.
- Region IV: Since  $\Phi > \Phi_c$  in this region, there is only one branch for the BI-AdS black holes. The free energies of the black hole with  $\tilde{a} = 0.1$  and  $\Phi = 35$  and the thermal AdS space are plotted in Fig. 3d. As in Region III, Large BH is the only global stable phase, and there is no phase transition.

The phase diagram in the  $\Phi - \tilde{T}$  space of the BI-AdS black hole with  $\tilde{a} = 0.1$  is displayed in the left panel of Fig. 4. There is a BH/thermal AdS first order phase transition line for some range of  $\Phi$  and a BH/thermal AdS zeroth order phase transition line for larger values of  $\Phi$ . These two phase transition lines meet and terminate at the black dot. Here, we simply use BH to denote large BH without causing any confusion. The phase diagram of the BI-AdS black hole with  $\tilde{a} = 10^{-5}$  is displayed in the right panel of Fig. 4, which is similar to the  $\tilde{a} = 0.1$  case. It is noteworthy that the zeroth

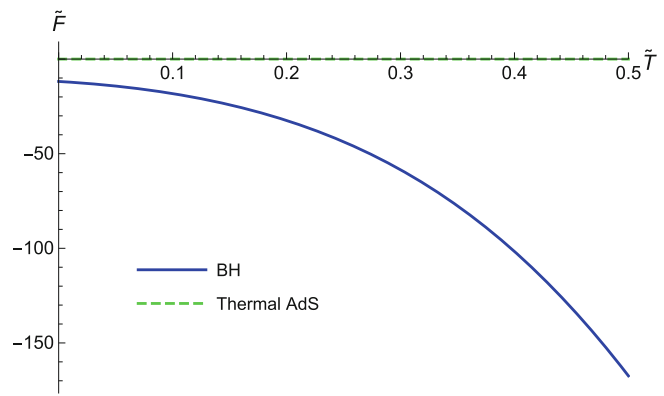


(a) Region I:  $\tilde{a} = 0.1$  and  $\Phi = 10$ . As  $\tilde{T}$  increases from zero, there is a first order phase transition occurring at the black dot from the thermal AdS space to Large BH.

(b) Region II:  $\tilde{a} = 0.1$  and  $\Phi = 25$ . As  $\tilde{T}$  increases from zero, there is a zeroth order phase transition occurring along the black dotted line from the thermal AdS space to Large BH.



(c) Region III:  $\tilde{a} = 0.1$  and  $\Phi = 32$ . There is no phase transition.



(d) Region IV:  $\tilde{a} = 0.1$  and  $\Phi = 35$ . There is no phase transition.

**Fig. 3** Plots of the free energy  $\tilde{F}$  against the temperature  $\tilde{T}$  for BI-AdS black holes in Regions I, II, III and IV. The black holes on the blue branches are thermally stable

order phase transition line becomes shorter for a smaller value of  $\tilde{a}$ . For a RN-AdS black hole, which has  $\tilde{a} = 0$ , there is no zeroth order phase transition [42].

### 3 Born–Infeld black holes in a cavity

In this section, we consider a thermodynamic system with Born–Infeld electrodynamics charged black holes inside a cavity, on the boundary of which the temperature and the potential are fixed. On a  $(3 + 1)$  dimensional spacetime manifold  $\mathcal{M}$  with a time-like boundary  $\partial\mathcal{M}$ , the action is given by

$$S = \int_{\mathcal{M}} d^4x \sqrt{-g} [R + \mathcal{L}_{\text{BI}}(F)] - 2 \int_{\partial\mathcal{M}} d^3x \sqrt{-\gamma} (K - K_0), \tag{11}$$

where  $K$  is the extrinsic curvature,  $\gamma$  is the metric on the boundary, and  $K_0$  is a subtraction term to make the boundary term vanish in flat spacetime. The BI black hole solution of the action (11) is [63]

$$ds^2 = -f(r) dt^2 + \frac{dr^2}{f(r)} + r^2 (d\theta^2 + \sin^2 \theta d\phi^2),$$

$$A = A_t(r) dt, \tag{12}$$

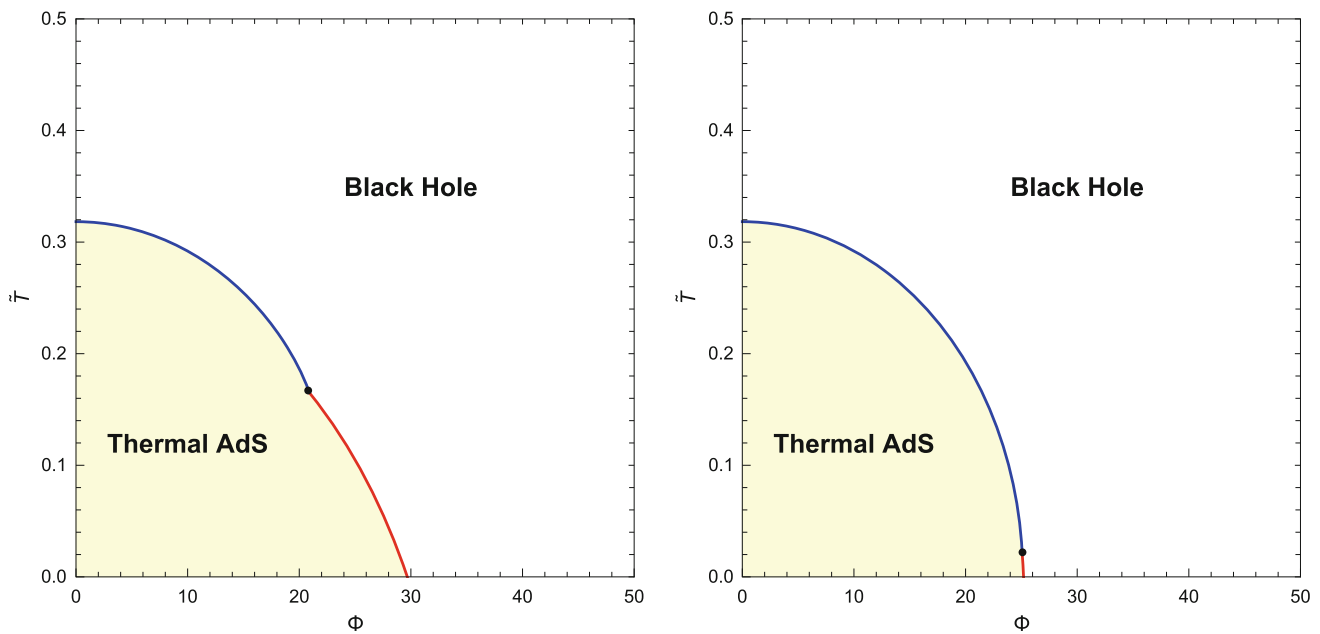


**Fig. 4** The phase diagrams of BI-AdS black holes in the  $\Phi$ - $\tilde{T}$  phase space. Left panel:  $\tilde{a} = 0.1$ . Right panel:  $\tilde{a} = 10^{-5}$ . The first/zeroth order phase transition lines separating the black holes and the thermal

AdS space are displayed by the blue/red lines. The first and zeroth order phase transition lines meet and terminate at the black dots

where

$$f(r) = 1 - \frac{M}{8\pi r} - \frac{Q^2}{6\sqrt{r^4 + aQ^2} + 6r^2} + \frac{Q^2}{3r^2} {}_2F_1\left(\frac{1}{4}, \frac{1}{2}, \frac{5}{4}; -\frac{aQ^2}{r^4}\right),$$

$$A'_t(r) = \frac{Q}{\sqrt{r^4 + aQ^2}}. \tag{13}$$

Here  $M$  and  $Q$  are the mass and the charge of the back hole, respectively. Note that  $M$  plays no role in our paper since we always use the horizon radius  $r_+$  to eliminate  $M$ .

Suppose that the wall of the cavity enclosing the BI black holes is at  $r = r_B$ , and the wall is maintained at a temperature of  $T$  and a gauge potential of  $\Phi$ , where we assume that  $\Phi > 0$  without loss of generality. For this system, the Euclidean continuation of the action  $\mathcal{S}$  was calculated in [63]:

$$\mathcal{S}^E = \frac{16\pi r_B}{T} \left[ 1 - \sqrt{f(r_B)} \right] - S - \frac{Q\Phi}{T}, \tag{14}$$

where  $S = 16\pi^2 r_+^2$  is the entropy of the black hole. In the semiclassical approximation, the free energy  $F$  is related to  $\mathcal{S}^E$  by

$$F = T\mathcal{S}^E. \tag{15}$$

Expressing the mass  $M$  in terms of the horizon radius  $r_+$ , one finds that the free energy  $F$  is a function of the temperature

$T$ , the potential  $\Phi$ , the charge  $Q$ , the cavity radius  $r_B$  and the horizon radius  $r_+$ :

$$F = F(r_+, Q; T, \Phi, r_B), \tag{16}$$

where  $T$ ,  $\Phi$  and  $r_B$  are parameters of the grand canonical ensemble. The locally stationary points of the free energy  $F$  can be determined by extremizing  $F(r_+, Q; T, \Phi, r_B)$  with respect to  $r_+$  and  $Q$ :

$$\frac{dF(r_+, Q; T, \Phi, r_B)}{dr_+} = 0 \implies T = \frac{T_h}{\sqrt{f(r_B)}},$$

$$\frac{dF(r_+, Q; T, \Phi, r_B)}{dQ} = 0 \implies \Phi = \frac{4\pi A_t(r_B)}{\sqrt{f(r_B)}}, \tag{17}$$

where

$$T_h = \frac{1}{4\pi r_+} \left( 1 - \frac{1}{2} \frac{Q^2}{r_+^2 + \sqrt{r_+^4 + aQ^2}} \right), \tag{18}$$

is the Hawking temperature of the black hole. Usually, it is convenient to express quantities in units of  $r_B$ :

$$x \equiv \frac{r_+}{r_B}, \tilde{Q} \equiv \frac{Q}{r_B}, \tilde{a} \equiv \frac{a}{r_B^2}, \tilde{T} \equiv r_B T \text{ and } \tilde{F} = \frac{F}{16\pi r_B}. \tag{19}$$



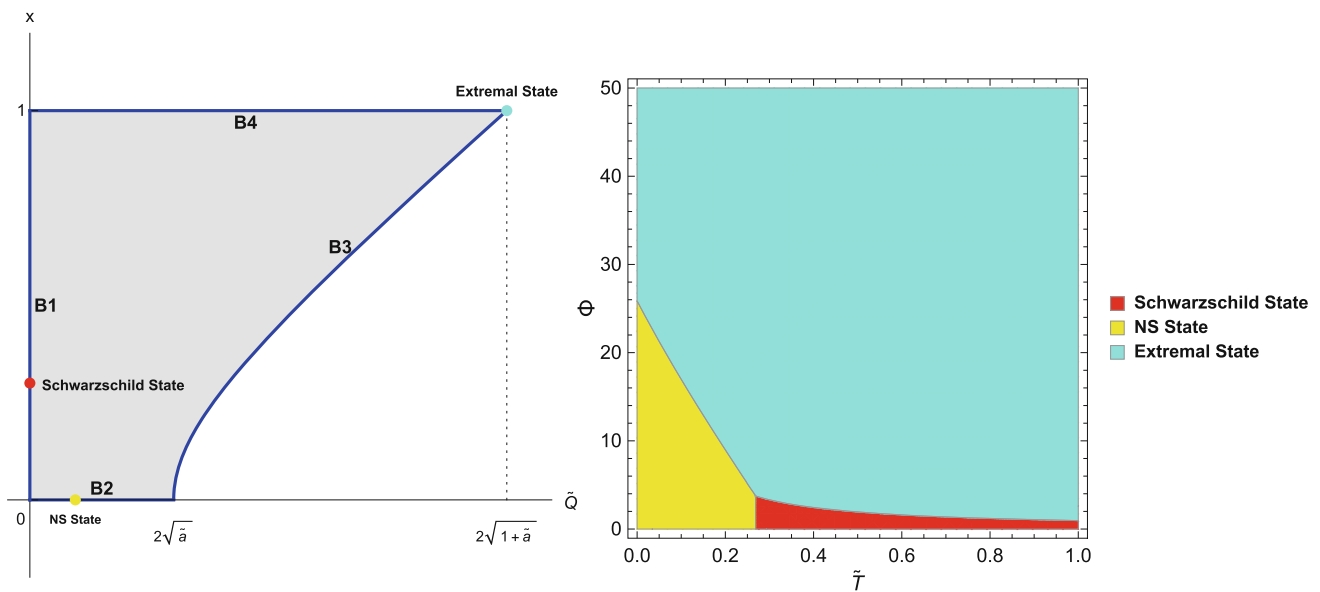


**Fig. 5** Left panel: Physically allowed values of  $x$  and  $\tilde{Q}$  for BI black holes in a cavity. The blue lines are the boundaries, on which the colored dots represent the candidates for the global minimum state of the free energy on the boundaries. Right panel: Global minimum state of the

free energy on the boundaries in the  $\tilde{T}$ - $\Phi$  space with  $\tilde{a} = 0.1$ . Only NS state and Extremal State can be the global minimum state on the whole physical region

The potential  $\Phi$  is dimensionless. In terms of  $x$  and tilde quantities,  $f(r_B)$  and  $\tilde{F}$  can be expressed as

$$\begin{aligned}
 f(x) &= 1 - x + \frac{x\tilde{Q}^2}{6\sqrt{x^4 + \tilde{a}\tilde{Q}^2 + 6x^2}} \\
 &\quad - \frac{\tilde{Q}^2}{3x} {}_2F_1\left(\frac{1}{4}, \frac{1}{2}, \frac{5}{4}; -\frac{\tilde{a}\tilde{Q}^2}{x^4}\right) \\
 &\quad - \frac{\tilde{Q}^2}{6\sqrt{1 + \tilde{a}\tilde{Q}^2 + 6}} + \frac{\tilde{Q}^2}{3} {}_2F_1\left(\frac{1}{4}, \frac{1}{2}, \frac{5}{4}; -\tilde{a}\tilde{Q}^2\right), \\
 \tilde{F} &= \tilde{F}(x, \tilde{Q}; \tilde{T}, \Phi) = 1 - \sqrt{f(x)} - \pi x^2 \tilde{T} - \frac{\tilde{Q}\Phi}{16\pi}, \tag{20}
 \end{aligned}$$

respectively.

For the BI black holes residing in a cavity, there appears to be some constraints imposed on  $x$  and  $\tilde{Q}$ . As shown in [63], when  $\tilde{Q}^2 < 4\tilde{a}$ , BI black holes are Schwarzschild-like type, which exist for  $0 < r_+ < r_B$ , or  $0 < x < 1$  in tilde variables. When  $\tilde{Q}^2 \geq 4\tilde{a}$ , BI black holes are RN type, which can have the extremal BI black hole solution with the nonzero horizon radius  $r_e = \sqrt{\tilde{Q}^2 - 4\tilde{a}}/2$ . Requiring that  $r_e < r_+ < r_B$  leads to  $\sqrt{\tilde{Q}^2 - 4\tilde{a}}/2 < x < 1$  and  $\tilde{Q}^2 \leq 4(1 + \tilde{a})$ . The physically allowed region for  $x$  and  $\tilde{Q}$  is depicted as the gray area in the left panel of Fig. 5. To determine the phase structures and transitions of a BI black hole residing in a cavity, we should find the local and global minima of the

free energy over the physically allowed region of  $x$  and  $\tilde{Q}$ . Solve Eq. (17) for  $x$  and  $\tilde{Q}$  gives the possible local minima of the free energy in the  $x$ - $\tilde{Q}$  space. However, one also needs to evaluate the free energy on the boundaries of the physically allowed region of  $x$  and  $\tilde{Q}$  to determine the global minimum:

- **B1:**  $0 \leq x \leq 1$  and  $\tilde{Q} = 0$ . The global minimum of the free energy on B1 is at  $x = 0$  when  $\tilde{T} < T_{B1c} \approx 0.2686$  and at  $x = x_{B1min} > 0$  otherwise. When  $\tilde{Q} = 0$  and  $x = 0$ , the boundary state is just the thermal flat space. The boundary state with  $\tilde{Q} = 0$  and  $x = x_{B1min}$  is a Schwarzschild black hole in a cavity, which is dubbed as Schwarzschild State. However, one finds that

$$\frac{\partial \tilde{F}}{\partial \tilde{Q}}|_{B1} = -\frac{\Phi}{16\pi} < 0, \tag{21}$$

which means that neither the thermal flat space nor Schwarzschild State can be the global minimum of the free energy over the whole physical region of  $x$  and  $\tilde{Q}$ .

- **B2:**  $x = 0$  and  $0 \leq \tilde{Q} \leq 2\sqrt{\tilde{a}}$ . For the state on B2, its metric and Ricci scalar are

$$f(r) = 1 - \frac{Q}{2\sqrt{a}} + \mathcal{O}(r) \text{ and } R = \frac{Q}{\sqrt{a}r^2} - \frac{2}{a} + \mathcal{O}(r), \tag{22}$$

respectively. Although the metric is regular, the space-time has a physical singularity at  $r = 0$ . So the state on B2

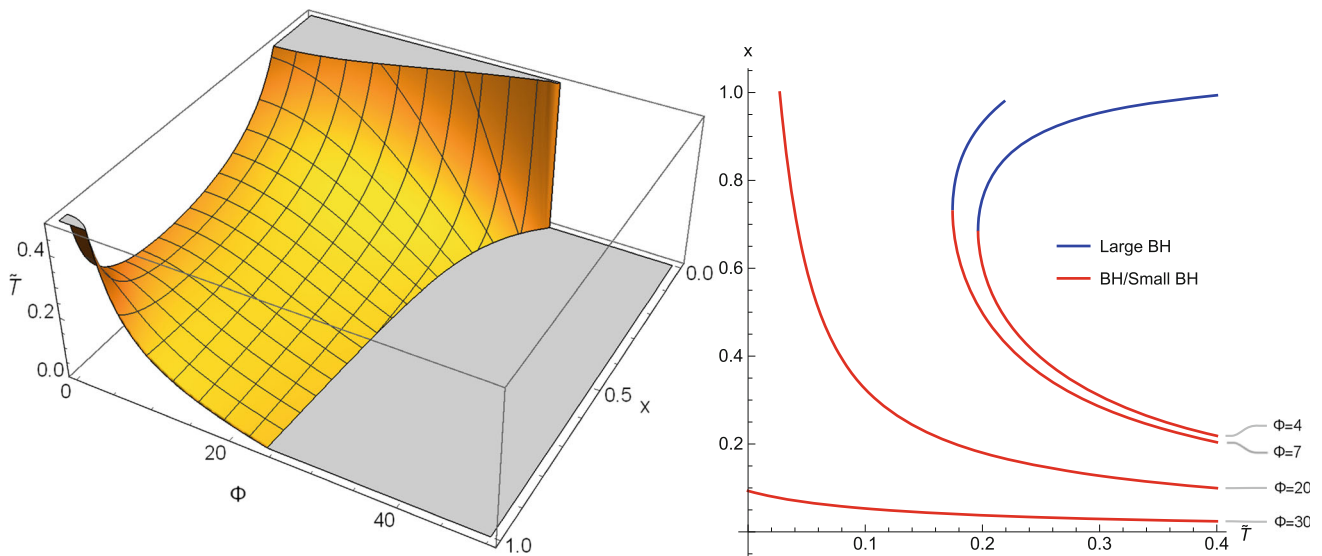


**Fig. 6** Plots of  $\tilde{T}(x, \Phi)$  and  $x(\tilde{T}, \Phi)$  for BI black holes at locally stationary points. Here  $\tilde{a} = 0.1$ . Left panel: plot of  $\tilde{T}$  as a function of  $x$  and  $\Phi$ .  $\tilde{T}$  is negative in the gray area. Right panel: plot of  $x$  against  $\tilde{T}$  for various values of  $\Phi$ . The blue/red branches are thermally stable/unstable

is a naked singularity since it has no horizon. The global minimum of the free energy on  $B2$  is at  $\tilde{Q} = \tilde{Q}_{B2min}$  with  $0 < \tilde{Q}_{B2min} < 2\sqrt{\tilde{a}}$  when  $\Phi \leq \Phi_{B2c}$  and at  $\tilde{Q} = 2\sqrt{\tilde{a}}$  otherwise. For simplicity, we denote the boundary state at  $\tilde{Q} = \tilde{Q}_{B2min}$  and  $x = 0$  as NS State. Note that the thermal flat space, which is at  $\tilde{Q} = 0$  and  $x = 0$  on  $B2$ , is never the global minimum of the free energy on  $B2$ .

- **B3:**  $x = \frac{1}{2}\sqrt{\tilde{Q}^2 - 4\tilde{a}}$  and  $2\sqrt{\tilde{a}} \leq \tilde{Q} \leq 2\sqrt{1 + \tilde{a}}$ . The boundary state on  $B3$  is an extremal BI black hole. In particular, the boundary state at  $\tilde{Q} = 2\sqrt{1 + \tilde{a}}$  and  $x = 1$  corresponds to the extremal BI black hole with the horizon merging with the wall of the cavity. We denote this state as Extremal State. It shows that the free energy can not have a local minimum on  $B3$  so the global minimum of the free energy on  $B3$  is either at  $\tilde{Q} = 2\sqrt{\tilde{a}}$  and  $x = 0$  or  $\tilde{Q} = 2\sqrt{1 + \tilde{a}}$  and  $x = 1$ .
- **B4:**  $x = 1$  and  $0 \leq \tilde{Q} \leq 2\sqrt{1 + \tilde{a}}$ . For a black hole on  $B4$ , the event horizon merges with the wall of the cavity. On  $B4$ ,  $\partial\tilde{F}/\partial\tilde{Q} = -\Phi/16\pi < 0$ , and hence the global minimum of the free energy on  $B4$  is at  $\tilde{Q} = 2\sqrt{1 + \tilde{a}}$ , which corresponds to Extremal State.

We find that the global minimum of the free energy on the four boundaries can only occur at Schwarzschild State, NS State or Extremal State, depending on the values of  $\tilde{a}$ ,  $\tilde{T}$  and  $\Phi$ . In the right panel of Fig. reffig:CB, the global minimum state on the boundaries is plotted in the  $\tilde{T}$ - $\Phi$  space with  $\tilde{a} = 0.1$ . As discussed above, only NS State and Extremal State are the candidates for the global minimum state on the physical region of  $x$  and  $\tilde{Q}$ .

The black hole at the locally stationary points of the free energy can remain in thermal equilibrium at constant tem-

perature and potential in a cavity. To determine the horizon radius of the black hole, we need to solve Eq. (17) for  $x$  in terms of  $\tilde{T}$  and  $\Phi$ :  $x(\tilde{T}, \Phi)$ . If  $x(\tilde{T}, \Phi)$  is multivalued, there are more than one branch of different sizes. As  $x \rightarrow 0$ , we find that there is a critical potential  $\Phi_{c1}$  such that  $\tilde{T} \rightarrow +\infty (-\infty)$  when  $\Phi < \Phi_{c1} (\Phi > \Phi_{c1})$ . As  $x \rightarrow 1$ , one has that

$$\tilde{T} \sim \frac{\Phi_{c2}^2 - \Phi^2}{32\pi^2\sqrt{1 + a\Phi}}, \tag{23}$$

where  $\Phi_{c2} = \frac{8\sqrt{1+a\pi}}{\sqrt{1+2a}} < \Phi_{c1}$ . Therefore at  $x = 1$ ,  $\tilde{T} > 0 (< 0)$  when  $\Phi < \Phi_{c2} (\Phi > \Phi_{c2})$ . We also find that, for  $\Phi > \Phi_{c1}$ ,  $\tilde{T}$  is always negative, and hence  $\tilde{F}$  has no locally stationary points. When  $\Phi_{c2} < \Phi < \Phi_{c1}$ , it can show that  $\tilde{T}$  is monotonic as a function of  $x$ , which means that there is only one branch of black holes with fixed values of  $\tilde{T}$  and  $\Phi$ . In the left panel of Fig. 6, we plot  $\tilde{T}$  as a function of  $x$  and  $\Phi$  with  $\tilde{a} = 0.1$ , which shows that  $\tilde{T}$  is negative for large enough value of  $\Phi$ , as expected. We also plot  $x$  against  $\tilde{T}$  for various values of  $\Phi$  with  $\tilde{a} = 0.1$  in the right panel of Fig. 6. When  $\Phi = 4$  and  $7$ , there are two family of black holes of different sizes with the same values of  $\tilde{T}$  and  $\Phi$ : small BH and and large BH. When  $\Phi = 20 < \Phi_{c2}$ ,  $\tilde{T} > 0$  at  $x = 1$  and there is only one branch: BH. When  $\Phi = 30 > \Phi_{c2}$ , there is still only one branch, on which there exists an extremal black hole at  $\tilde{T} = 0$ . Since thermally stable phases have  $\partial x/\partial\tilde{T} > 0$ , the BI black holes on blue/red branches are thermally stable/unstable.

Evaluating the free energy both on the boundaries and at the locally stationary points, we find that there are four regions in the  $\tilde{a}$ - $\Phi$  phase space, in each of which the the



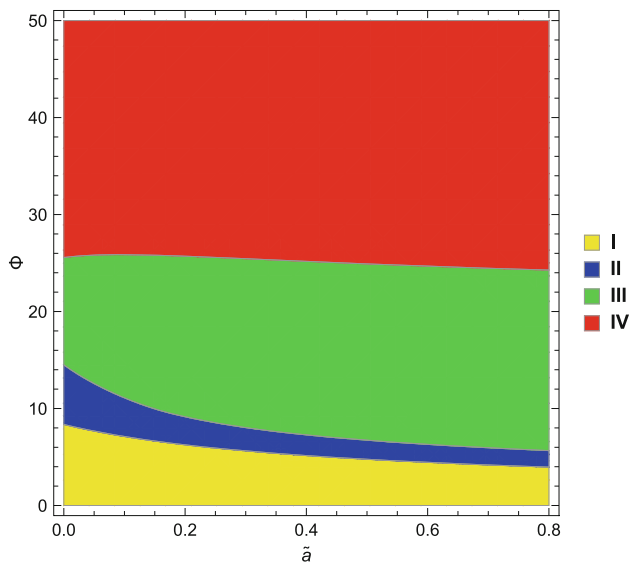


**Fig. 7** The four regions in the  $\tilde{a}$ - $\Phi$  space of the systems with BI black holes enclosed in a cavity, each of which possesses distinct behavior of the phase structures and transitions. Varying the temperature, a first order NS State/Large BH phase transition and a second order Large BH/Extremal State phase transition occur in Regions I, while only a first order NS State/Extremal State phase transition occurs in Regions II and III. There is no phase transition in Regions IV

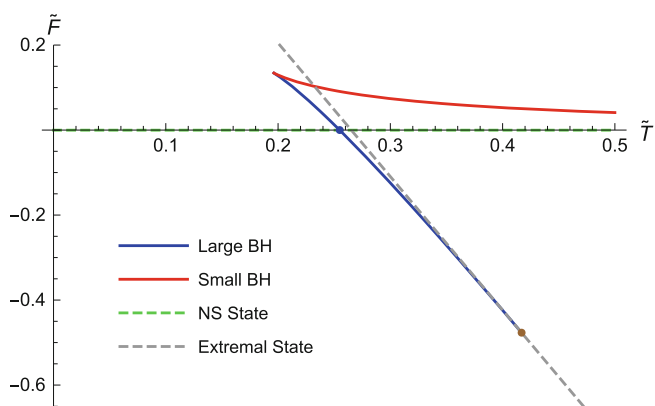
system have different phase structures and transitions. These four regions of the  $\tilde{a}$ - $\Phi$  phase space are mapped in Fig. 7. In what follows, we discuss the system in the four regions:

- **Region I:** There is a temperature of  $\tilde{T}_{\min} > 0$ , above which black holes at the locally stationary points have two branches: Large BH and Small BH. The Large/Small BH branch is thermally stable/unstable. The free energies of the two branches, NS State and Extremal State are plotted in Fig. 8a, where  $\tilde{a} = 0.1$  and  $\Phi = 4$ . For  $\tilde{T} < \tilde{T}_{\min}$ , there are no locally stationary points, and the global minimum of the free energy is at NS State. At  $\tilde{T} = \tilde{T}_{\min}$ , locally stationary points start to appear. As  $\tilde{T}$  increases from  $\tilde{T}_{\min}$ , the free energy of Large BH decrease while that of NS state is constant. They cross each other at the blue dot, where a first order phase transition occurs. Further increasing  $\tilde{T}$ , Large BH stays globally stable until it terminates and merge into Extremal State at the brown dot. At the brown dot, Large BH and Extremal State both have  $x = 1$ , and the entropy is continuous across the transition. So the phase transition occurring at the brown dot is a second order one, after which Extremal State becomes the globally minimum state.
- **Region II:** As in Region I, the free energy has no locally stationary points, and the global minimum state is NS state when  $\tilde{T} < \tilde{T}_{\min}$ . The locally stationary points of the free energy emerge when  $\tilde{T} > \tilde{T}_{\min}$ , which consist of one thermally stable branch and one or two thermally

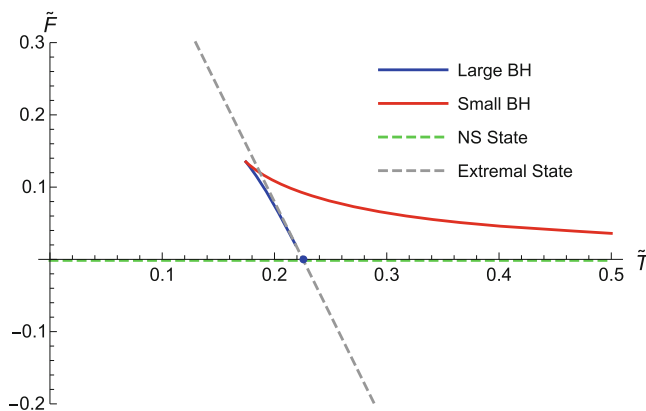
unstable branches. When there are two branches of black holes, the free energies of the two branches, NS State and Extremal State are plotted in Fig. 8b, where  $\tilde{a} = 0.1$  and  $\Phi = 7$ . It shows that there seems to be a second order phase transition from Large BH to Extremal State. However, the Large BH branch and the second order phase transition are never the global minimum. So we only have a first order phase transition from NS State to Extremal State occurring at the blue dot. In this region, the black holes at the locally stationary points could also have three branches, which are plotted in the left panel of Fig. 9. Only Intermediate BH is thermally stable. The free energies of the three branches, NS State and Extremal State are plotted in the right panel of Fig. 9, where  $\tilde{a} = 0.7$  and  $\Phi = 5.5$ . It shows that, as  $\tilde{T}$  increases, the global minimum also experiences a first order phase transition from NS State to Extremal State. The inset in the right panel of Fig. 9 illustrates that the phase transition from Intermediate BH to Extremal State is first order due to the existence of Large BH.

- **Region III:** The locally stationary points only consist of one thermally unstable branch, which can never be the global minimum. The free energies of the unstable branch, NS State and Extremal State are plotted in Fig. 8c, where  $\tilde{a} = 0.1$  and  $\Phi = 20$ . The global minimum state is NS state for low temperatures and Extremal State for high temperatures. A first order phase transitions occurs at the blue dot.
- **Region IV:** When  $\Phi < \Phi_{c1}$ , the locally stationary points exist and have only one branch of thermally unstable black holes. The free energies of the unstable branch, NS State and Extremal State are plotted in Fig. 8c, where  $\tilde{a} = 0.1$  and  $\Phi = 30$ . Extremal State is the only global stable phase, and there is no phase transition. When  $\Phi > \Phi_{c1}$ , there are no locally stationary points for the free energy, and Extremal State is the only globally stable phase as well.

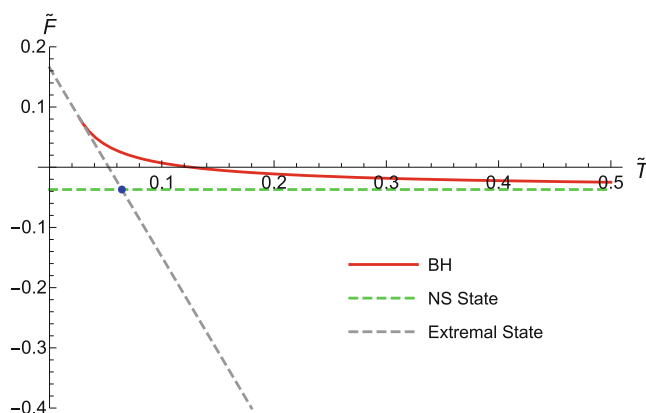
In Fig. 10, the globally stable phase diagram of the system with  $\tilde{a} = 0.1$  is displayed in the  $\Phi$ - $\tilde{T}$  phase space. For NS State and Extremal State, the system admits a globally stable phase on the boundaries of the physical  $x$  and  $\tilde{Q}$  region. As discussed above, there is no more than one thermally stable branch of BI black holes at the locally stationary points. So the system admits at most one locally stable phase, which describes a BI black hole in thermally stable equilibrium in a cavity and is denoted by BH. The BH phase occurs in the phase diagram when it is globally stable. There is a BH/NS State first order phase transition for some range of  $\Phi$ , a NS State/Extremal State first order phase transition for some smaller range of  $\Phi$  and a BH/Extremal State second order phase transition for some larger range of  $\Phi$ . These three phase transition lines merge together at the black dot.



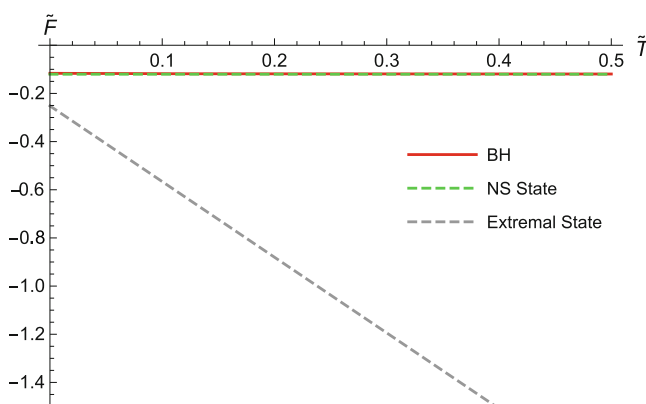
(a) Region I:  $\tilde{a} = 0.1$  and  $\Phi = 4$ . As  $\tilde{T}$  increases from zero, a first order phase transition from NS State to Large BH occurs at the blue dot. Further increasing  $\tilde{T}$ , there will be a second order phase transition from Large BH to Extremal State at the brown dot.



(b) Region II:  $\tilde{a} = 0.1$  and  $\Phi = 7$ . As  $\tilde{T}$  increases from zero, there is a first order phase transition at the blue dot from NS State to Extremal State. The second phase transition from Large BH to Extremal State is cloaked by NS State.



(c) Region III:  $\tilde{a} = 0.1$  and  $\Phi = 20$ . As the system is heated, it undergoes a first order phase transition from NS State to Extremal State.



(d) Region IV:  $\tilde{a} = 0.1$  and  $\Phi = 30$ . The globally stable phase only is Extremal State, and hence there is no phase transition.

**Fig. 8** Plots of the free energy  $\tilde{F}$  against the temperature  $\tilde{T}$  for different branches of BI black holes at the locally stationary points, NS State and Extremal State of the systems in Regions I, II, III and IV. The black

holes on the blue branches are thermally stable. The blue/brown dots represent first/second phase transitions of the globally stable phases

### 4 Discussion and conclusion

In this paper, we studied the phase structures and transitions of BI black holes in a grand canonical ensemble by considering two boundary conditions, namely the asymptotically AdS boundary and the Dirichlet boundary in the asymptotically flat spacetime. For BI-AdS black holes, the phase structure

with respect to  $\tilde{a}$  and  $\Phi$  was displayed in Fig. 2, where there are four regions. For fixed values of the potential  $\Phi$  and the temperature  $T$ , the black holes in Regions I, II and III admit two solutions of different sizes: Large BH (thermally stable) and Small BH (thermally unstable). In Region IV, there is only one branch of black hole solutions, which are thermally stable. In Fig. 4, the globally stable phases and the phase

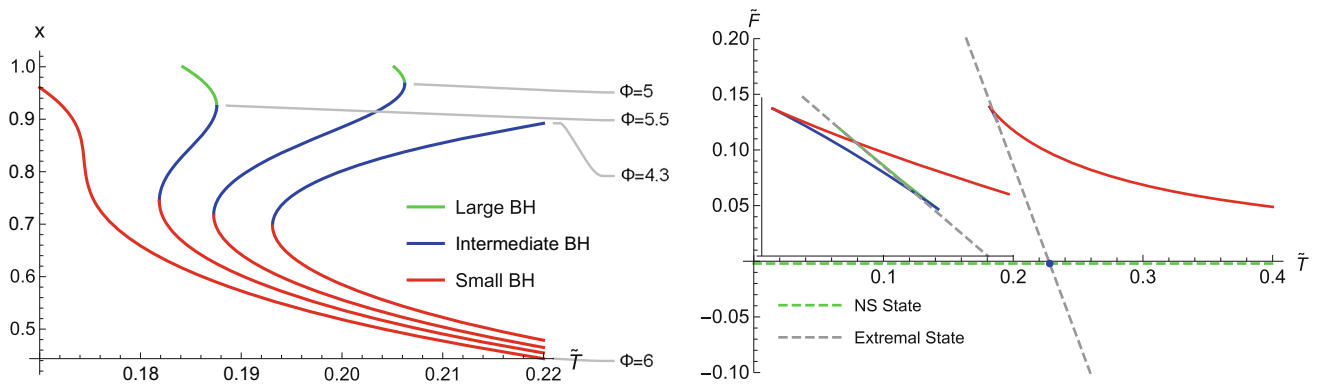


**Fig. 9** Left panel: plot of  $x$  against  $\tilde{T}$  for various values of  $\Phi$  with  $\tilde{a} = 0.7$ . Only the blue branches are thermally stable. The systems with  $\Phi = 5$  and  $5.5$  are in Region II, which have three branches of BI black

holes. Right panel: plot of  $\tilde{F}$  against  $\tilde{T}$  for the phases of the system with  $\Phi = 5.5$  and  $\tilde{a} = 0.7$ . As  $\tilde{T}$  increases, the system undergoes a first order transition from NS State to Extremal State

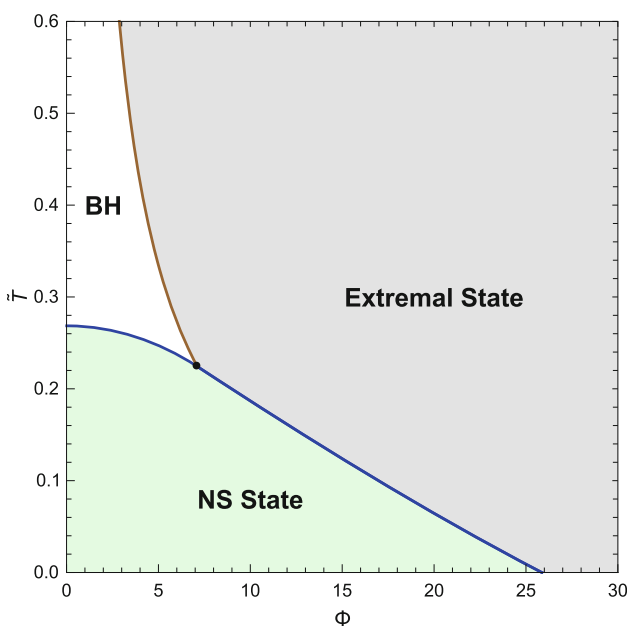


**Fig. 10** The globally stable phase diagram of the system with  $\tilde{a} = 0.1$  in the  $\Phi$ - $\tilde{T}$  space. The blue/brown line represents a first/second phase transition line. The three phase transitions merge at the black dot

transitions were shown in the  $\Phi$ - $\tilde{T}$  phase space. There are two the globally stable phases, which are BH and thermal AdS space. There are a BH/Thermal AdS zeroth order phase transition for some range of  $\Phi$  and a BH/Thermal AdS first order phase transition for smaller values of  $\Phi$ . Note that the local and global stabilities of BI-AdS black holes in the grand ensemble were already studied in [42], where the branches of BI-AdS black holes and the BH/Thermal AdS first and zeroth order phase transitions were found. In this paper, we investigated phase structures of BI-AdS black holes in the grand ensemble in a more thorough way. To our knowledge, the phase diagrams 2 and 4 has yet to be reported. Moreover, Region III of Fig. 2 was not observed in [42]. One can also

study the phase structures and transitions of BI-AdS black holes in the context of the extended phase space thermodynamics, where the cosmological constant is interpreted as thermodynamic pressure, i.e.,  $P = 6/l^2$  [13,64]. Our results can simply be generalized to the extended phase space case by making replacements

$$\tilde{T} = T\sqrt{6/P}, \tilde{a} = aP/6 \text{ and } \tilde{F} \equiv F\sqrt{P/6}. \tag{24}$$

To determine the phase structure of BI black holes in a cavity, we computed the locally stationary points of the free energy of the system over the physical parameter space and the global minimum on the corresponding boundaries. For the global minimum state on the boundaries, only NS State, which describes a naked singularity, and Extremal State, which describes an extremal black hole with the horizon merging with the wall of the cavity, are the candidates for the global minimum state on the whole physical region. The phase structure with respect to  $\tilde{a}$  and  $\Phi$  was displayed in Fig. 7, where there are also four regions. In Regions I and II, the system admits one locally (thermally) stable phase while there are one or two locally (thermally) unstable phases. The system in Region III and IV only has one locally (thermally) unstable phase. The phases of the system that have the globally minimum of the free energy were shown in Fig. 10, which are Black hole, NS State and Extremal State. The phase transitions between globally stable phases of the system were also represented in Fig. 10, which shows there occur a Hawking-Page-like transition between BH and NS State and a second-order phase transition between BH and Extremal State. In this paper, we only focus on spherical topology, and hence it is possible that there are some other states of lower free energy in a different topological sector with the same potential and temperature. If this happens, the globally stable phases discussed above could be only metastable.

For BI black holes in a cavity, the flat thermal space is on the boundary of the physical region of the system. However,

NS state or Extremal State is always preferred over the flat thermal space. So the flat thermal space is never the globally stable phase of the system. As shown in Fig. 8a, b, there are some regions of the parameter space, in which NS state is globally stable while there is an unstable branch of the BI black hole solution. Perturbing the unstable black hole, we find that the black hole radiates away more energy than it absorbs, and the system would eventually settle down to a naked singularity. Finding a time-dependent solution, which describes a BI black hole evolving to a naked singularity, is very tempting, since such solution can provide a counterexample to the weak cosmic censorship conjecture [65].

Finally, we found that, in the grand canonical ensemble, there are some dissimilarities between the phase structures and transitions of BI-AdS black hole and those of BI black holes in a cavity: (1) For BI-AdS black holes, the thermal AdS space is sometimes preferred over the black hole solutions. Inspired by the phase structure of RN black holes in a cavity [17], one would expect that, for BI black holes in a cavity, the thermal flat space could sometimes be globally preferred. However, our results showed that the thermal flat space is never globally preferred. Instead, NS state or Extremal State can be the globally minimum state. (2) Although a Hawking-Page-like first order phase transition occurs in both cases, the system admits a second order phase transition for BI black holes in a cavity and a zeroth order phase transition for BI-AdS black holes. (3) In some regions in the parameter space of BI black holes in a cavity, the system can have three locally extremal states of different sizes: one thermally stable one and two thermally unstable ones. On the other hand, BI-AdS black hole solutions have no more than two branches of different sizes.

**Acknowledgements** We are grateful to Zheng Sun and Zhipeng Zhang for useful discussions and valuable comments. This work is supported in part by NSFC (Grant nos. 11005016, 11175039 and 11375121).

**Data Availability Statement** This manuscript has no associated data or the data will not be deposited. [Authors' comment: The results of this paper are based on the theoretical derivation. We do not use any data in the calculations.]

**Open Access** This article is licensed under a Creative Commons Attribution 4.0 International License, which permits use, sharing, adaptation, distribution and reproduction in any medium or format, as long as you give appropriate credit to the original author(s) and the source, provide a link to the Creative Commons licence, and indicate if changes were made. The images or other third party material in this article are included in the article's Creative Commons licence, unless indicated otherwise in a credit line to the material. If material is not included in the article's Creative Commons licence and your intended use is not permitted by statutory regulation or exceeds the permitted use, you will need to obtain permission directly from the copyright holder. To view a copy of this licence, visit <http://creativecommons.org/licenses/by/4.0/>.  
Funded by SCOAP<sup>3</sup>.

## References

1. S.W. Hawking, Particle creation by black holes, *Commun. Math. Phys.* **43**, 199 (1975). Erratum: [*Commun. Math. Phys.* **46**, 206 (1976)]. <https://doi.org/10.1007/BF01608497>
2. J.D. Bekenstein, Black holes and the second law. *Lett. Nuovo Cim.* **4**, 737 (1972). <https://doi.org/10.1007/BF02757029>
3. J.D. Bekenstein, Black holes and entropy. *Phys. Rev. D* **7**, 2333 (1973). <https://doi.org/10.1103/PhysRevD.7.2333>
4. S.W. Hawking, D.N. Page, Thermodynamics of black holes in anti-De Sitter space. *Commun. Math. Phys.* **87**, 577 (1983). <https://doi.org/10.1007/BF01208266>
5. J.M. Maldacena, The large N limit of superconformal field theories and supergravity, *Int. J. Theor. Phys.* **38**, 1113 (1999). [*Adv. Theor. Math. Phys.* **2**, 231 (1998)] <https://doi.org/10.1023/A:1026654312961>, <https://doi.org/10.4310/ATMP.1998.v2.n2.a1> [arXiv:hep-th/9711200]
6. S.S. Gubser, I.R. Klebanov, A.M. Polyakov, Gauge theory correlators from noncritical string theory. *Phys. Lett. B* **428**, 105 (1998). [https://doi.org/10.1016/S0370-2693\(98\)00377-3](https://doi.org/10.1016/S0370-2693(98)00377-3) [arXiv:hep-th/9802109]
7. E. Witten, Anti-de Sitter space and holography. *Adv. Theor. Math. Phys.* **2**, 253 (1998). <https://doi.org/10.4310/ATMP.1998.v2.n2.a2> [arXiv:hep-th/9802150]
8. E. Witten, Anti-de Sitter space, thermal phase transition, and confinement in gauge theories. *Adv. Theor. Math. Phys.* **2**, 505 (1998). <https://doi.org/10.4310/ATMP.1998.v2.n3.a3> [arXiv:hep-th/9803131]
9. A. Chamblin, R. Emparan, C.V. Johnson, R.C. Myers, Charged AdS black holes and catastrophic holography. *Phys. Rev. D* **60**, 064018 (1999). <https://doi.org/10.1103/PhysRevD.60.064018> [arXiv:hep-th/9902170]
10. A. Chamblin, R. Emparan, C.V. Johnson, R.C. Myers, Holography, thermodynamics and fluctuations of charged AdS black holes. *Phys. Rev. D* **60**, 104026 (1999). <https://doi.org/10.1103/PhysRevD.60.104026> [arXiv:hep-th/9904197]
11. M.M. Caldarelli, G. Cognola, D. Klemm, Thermodynamics of Kerr–Newman-AdS black holes and conformal field theories. *Class. Quantum Gravity* **17**, 399 (2000). <https://doi.org/10.1088/0264-9381/17/2/310> [arXiv:hep-th/9908022]
12. R.G. Cai, Gauss–Bonnet black holes in AdS spaces. *Phys. Rev. D* **65**, 084014 (2002). <https://doi.org/10.1103/PhysRevD.65.084014> [arXiv:hep-th/0109133]
13. D. Kubiznak, R.B. Mann, P–V criticality of charged AdS black holes. *JHEP* **1207**, 033 (2012). [https://doi.org/10.1007/JHEP07\(2012\)033](https://doi.org/10.1007/JHEP07(2012)033) [arXiv:1205.0559 [hep-th]]
14. J.W. York Jr., Black hole thermodynamics and the Euclidean Einstein action. *Phys. Rev. D* **33**, 2092 (1986). <https://doi.org/10.1103/PhysRevD.33.2092>
15. H.W. Braden, J.D. Brown, B.F. Whiting, J.W. York Jr., Charged black hole in a grand canonical ensemble. *Phys. Rev. D* **42**, 3376 (1990). <https://doi.org/10.1103/PhysRevD.42.3376>
16. S. Carlip, S. Vaidya, Phase transitions and critical behavior for charged black holes. *Class. Quantum Gravity* **20**, 3827 (2003). <https://doi.org/10.1088/0264-9381/20/16/319> [arXiv:gr-qc/0306054]
17. A.P. Lundgren, Charged black hole in a canonical ensemble. *Phys. Rev. D* **77**, 044014 (2008). <https://doi.org/10.1103/PhysRevD.77.044014> [arXiv:gr-qc/0612119]
18. J.X. Lu, S. Roy, Z. Xiao, Phase transitions and critical behavior of black branes in canonical ensemble. *JHEP* **1101**, 133 (2011). [https://doi.org/10.1007/JHEP01\(2011\)133](https://doi.org/10.1007/JHEP01(2011)133) [arXiv:1010.2068 [hep-th]]



19. C. Wu, Z. Xiao, J. Xu, Bubbles and black branes in grand canonical ensemble. *Phys. Rev. D* **85**, 044009 (2012). <https://doi.org/10.1103/PhysRevD.85.044009> [arXiv:1108.1347 [hep-th]]
20. J.X. Lu, R. Wei, J. Xu, The phase structure of black D1/D5 (F/NS5) system in canonical ensemble. *JHEP* **1212**, 012 (2012). [https://doi.org/10.1007/JHEP12\(2012\)012](https://doi.org/10.1007/JHEP12(2012)012) [arXiv:1210.0708 [hep-th]]
21. J.X. Lu, R. Wei, Modulating the phase structure of black D6 branes in canonical ensemble. *JHEP* **1304**, 100 (2013). [https://doi.org/10.1007/JHEP04\(2013\)100](https://doi.org/10.1007/JHEP04(2013)100) [arXiv:1301.1780 [hep-th]]
22. D. Zhou, Z. Xiao, Phase structures of the black  $Dp - D(p + 4)$ -brane system in various ensembles I: thermal stability. *JHEP* **1507**, 134 (2015). [https://doi.org/10.1007/JHEP07\(2015\)134](https://doi.org/10.1007/JHEP07(2015)134) [arXiv:1502.00261 [hep-th]]
23. Z. Xiao, D. Zhou, Phase structures of the black  $Dp - D(p + 4)$ -brane system in various ensembles II: electrical and thermodynamic stability. *JHEP* **1509**, 028 (2015). [https://doi.org/10.1007/JHEP09\(2015\)028](https://doi.org/10.1007/JHEP09(2015)028) [arXiv:1507.02088 [hep-th]]
24. P. Basu, C. Krishnan, P.N.B. Subramanian, Hairy black holes in a box. *JHEP* **1611**, 041 (2016). [https://doi.org/10.1007/JHEP11\(2016\)041](https://doi.org/10.1007/JHEP11(2016)041) [arXiv:1609.01208 [hep-th]]
25. Y. Peng, B. Wang, Y. Liu, On the thermodynamics of the black hole and hairy black hole transitions in the asymptotically flat spacetime with a box. *Eur. Phys. J. C* **78**(3), 176 (2018). <https://doi.org/10.1140/epjc/s10052-018-5652-0> [arXiv:1708.01411 [hep-th]]
26. Y. Peng, Studies of a general flat space/boson star transition model in a box through a language similar to holographic superconductors. *JHEP* **1707**, 042 (2017). [https://doi.org/10.1007/JHEP07\(2017\)042](https://doi.org/10.1007/JHEP07(2017)042) [arXiv:1705.08694 [hep-th]]
27. Y. Peng, Scalar field configurations supported by charged compact reflecting stars in a curved spacetime. *Phys. Lett. B* **780**, 144 (2018). <https://doi.org/10.1016/j.physletb.2018.02.068> [arXiv:1801.02495 [gr-qc]]
28. N. Sanchis-Gual, J.C. Degollado, P.J. Montero, J.A. Font, C. Herdeiro, Explosion and final state of an unstable Reissner–Nordstrom black hole. *Phys. Rev. Lett.* **116**(14), 141101 (2016). <https://doi.org/10.1103/PhysRevLett.116.141101> [arXiv:1512.05358 [gr-qc]]
29. S.R. Dolan, S. Ponglertsakul, E. Winstanley, Stability of black holes in Einstein-charged scalar field theory in a cavity. *Phys. Rev. D* **92**(12), 124047 (2015). <https://doi.org/10.1103/PhysRevD.92.124047> [arXiv:1507.02156 [gr-qc]]
30. S. Ponglertsakul, E. Winstanley, S.R. Dolan, Stability of gravitating charged-scalar solitons in a cavity. *Phys. Rev. D* **94**(2), 024031 (2016). <https://doi.org/10.1103/PhysRevD.94.024031> [arXiv:1604.01132 [gr-qc]]
31. N. Sanchis-Gual, J.C. Degollado, C. Herdeiro, J.A. Font, P.J. Montero, Dynamical formation of a Reissner–Nordstrom black hole with scalar hair in a cavity. *Phys. Rev. D* **94**(4), 044061 (2016). <https://doi.org/10.1103/PhysRevD.94.044061> [arXiv:1607.06304 [gr-qc]]
32. S. Ponglertsakul, E. Winstanley, Effect of scalar field mass on gravitating charged scalar solitons and black holes in a cavity. *Phys. Lett. B* **764**, 87 (2017). <https://doi.org/10.1016/j.physletb.2016.10.073> [arXiv:1610.00135 [gr-qc]]
33. N. Sanchis-Gual, J.C. Degollado, J.A. Font, C. Herdeiro, E. Radu, Dynamical formation of a hairy black hole in a cavity from the decay of unstable solitons. *Class. Quantum Gravity* **34**(16), 165001 (2017). <https://doi.org/10.1088/1361-6382/aa7d1f> [arXiv:1611.02441 [gr-qc]]
34. O.J.C. Dias, R. Masachs, Charged black hole bombs in a Minkowski cavity. *Class. Quantum Gravity* **35**(18), 184001 (2018). <https://doi.org/10.1088/1361-6382/aad70b> [arXiv:1801.10176 [gr-qc]]
35. O.J.C. Dias, R. Masachs, Evading no-hair theorems: hairy black holes in a Minkowski box. *Phys. Rev. D* **97**(12), 124030 (2018). <https://doi.org/10.1103/PhysRevD.97.124030> [arXiv:1802.01603 [gr-qc]]
36. F. Simovic, R.B. Mann, Critical phenomena of charged de Sitter Black holes in cavities. *Class. Quantum Gravity* **36**(1), 014002 (2019). <https://doi.org/10.1088/1361-6382/aaf445> [arXiv:1807.11875 [gr-qc]]
37. L. McGough, M. Mezei, H. Verlinde, Moving the CFT into the bulk with  $T\bar{T}$ . *JHEP* **1804**, 010 (2018). [https://doi.org/10.1007/JHEP04\(2018\)010](https://doi.org/10.1007/JHEP04(2018)010) [arXiv:1611.03470 [hep-th]]
38. M. Born, L. Infeld, Foundations of the new field theory. *Proc. R. Soc. Lond. A* **144**, 425 (1934). <https://doi.org/10.1098/rspa.1934.0059>
39. T.K. Dey, Born–Infeld black holes in the presence of a cosmological constant. *Phys. Lett. B* **595**, 484 (2004). <https://doi.org/10.1016/j.physletb.2004.06.047> [arXiv:hep-th/0406169]
40. R.G. Cai, D.W. Pang, A. Wang, Born–Infeld black holes in (A)dS spaces. *Phys. Rev. D* **70**, 124034 (2004). <https://doi.org/10.1103/PhysRevD.70.124034> [arXiv:hep-th/0410158]
41. S. Fernando, D. Krug, Charged black hole solutions in Einstein–Born–Infeld gravity with a cosmological constant. *Gen. Relativ. Gravit.* **35**, 129 (2003). <https://doi.org/10.1023/A:1021315214180> [arXiv:hep-th/0306120]
42. S. Fernando, Thermodynamics of Born–Infeld-anti-de Sitter black holes in the grand canonical ensemble. *Phys. Rev. D* **74**, 104032 (2006). <https://doi.org/10.1103/PhysRevD.74.104032> [arXiv:hep-th/0608040]
43. R. Banerjee, S. Ghosh, D. Roychowdhury, New type of phase transition in Reissner–Nordstrom–AdS black hole and its thermodynamic geometry. *Phys. Lett. B* **696**, 156 (2011). <https://doi.org/10.1016/j.physletb.2010.12.010> [arXiv:1008.2644 [gr-qc]]
44. R. Banerjee, D. Roychowdhury, Critical phenomena in Born–Infeld AdS black holes. *Phys. Rev. D* **85**, 044040 (2012). <https://doi.org/10.1103/PhysRevD.85.044040> [arXiv:1111.0147 [gr-qc]]
45. A. Lala, D. Roychowdhury, Ehrenfest’s scheme and thermodynamic geometry in Born–Infeld AdS black holes. *Phys. Rev. D* **86**, 084027 (2012). <https://doi.org/10.1103/PhysRevD.86.084027> [arXiv:1111.5991 [gr-qc]]
46. R. Banerjee, D. Roychowdhury, Critical behavior of Born–Infeld AdS black holes in higher dimensions. *Phys. Rev. D* **85**, 104043 (2012). <https://doi.org/10.1103/PhysRevD.85.104043> [arXiv:1203.0118 [gr-qc]]
47. S. Gunasekaran, R.B. Mann, D. Kubiznak, Extended phase space thermodynamics for charged and rotating black holes and Born–Infeld vacuum polarization. *JHEP* **1211**, 110 (2012). [https://doi.org/10.1007/JHEP11\(2012\)110](https://doi.org/10.1007/JHEP11(2012)110) [arXiv:1208.6251 [hep-th]]
48. D.C. Zou, S.J. Zhang, B. Wang, Critical behavior of Born–Infeld AdS black holes in the extended phase space thermodynamics. *Phys. Rev. D* **89**(4), 044002 (2014). <https://doi.org/10.1103/PhysRevD.89.044002> [arXiv:1311.7299 [hep-th]]
49. M. Azreg-Ainou, Black hole thermodynamics: no inconsistency via the inclusion of the missing  $P - V$  terms. *Phys. Rev. D* **91**, 064049 (2015). <https://doi.org/10.1103/PhysRevD.91.064049> [arXiv:1411.2386 [gr-qc]]
50. S.H. Hendi, B. Eslam Panah, S. Panahiyan, Einstein–Born–Infeld-massive gravity: adS-black hole solutions and their thermodynamical properties. *JHEP* **1511**, 157 (2015). [https://doi.org/10.1007/JHEP11\(2015\)157](https://doi.org/10.1007/JHEP11(2015)157) [arXiv:1508.01311 [hep-th]]
51. M. Kord Zangeneh, A. Dehyadegari, M.R. Mehdizadeh, B. Wang, A. Sheykhi, Thermodynamics, phase transitions and Ruppeiner geometry for Einstein–dilaton–Lifshitz black holes in the presence of Maxwell and Born–Infeld electrodynamics. *Eur. Phys. J. C* **77**(6), 423 (2017). <https://doi.org/10.1140/epjc/s10052-017-4989-0> [arXiv:1610.06352 [hep-th]]
52. X.X. Zeng, X.M. Liu, L.F. Li, Phase structure of the Born–Infeld-anti-de Sitter black holes probed by non-local observables.



- Eur. Phys. J. C **76**(11), 616 (2016). <https://doi.org/10.1140/epjcs10052-016-4463-4> [arXiv:1601.01160 [hep-th]]
53. S. Li, H. Lu, H. Wei, Dyonic (A)dS Black holes in Einstein–Born–Infeld theory in diverse dimensions. *JHEP* **1607**, 004 (2016). [https://doi.org/10.1007/JHEP07\(2016\)004](https://doi.org/10.1007/JHEP07(2016)004) [arXiv:1606.02733 [hep-th]]
54. S. Hossein Hendi, B. Eslam Panah, S. Panahiyan, M. Hassaine, BTZ dilatonic black holes coupled to Maxwell and Born–Infeld electrodynamics, *Phys. Rev. D* **98**(8), 084006 (2018). <https://doi.org/10.1103/PhysRevD.98.084006> [arXiv:1712.04328 [physics.gen-ph]]
55. A. Dehyadegari, A. Sheykhi, Reentrant phase transition of Born–Infeld–AdS black holes. *Phys. Rev. D* **98**(2), 024011 (2018). <https://doi.org/10.1103/PhysRevD.98.024011> [arXiv:1711.01151 [gr-qc]]
56. J. Tao, P. Wang, H. Yang, Testing holographic conjectures of complexity with Born–Infeld black holes. *Eur. Phys. J. C* **77**(12), 817 (2017). <https://doi.org/10.1140/epjcs10052-017-5395-3> [arXiv:1703.06297 [hep-th]]
57. X. Guo, P. Wang, H. Yang, Membrane paradigm and holographic DC conductivity for nonlinear electrodynamics. *Phys. Rev. D* **98**(2), 026021 (2018). <https://doi.org/10.1103/PhysRevD.98.026021> [arXiv:1711.03298 [hep-th]]
58. P. Wang, H. Wu, H. Yang, Thermodynamics and phase transitions of nonlinear electrodynamics black holes in an extended phase space, arXiv:1808.04506 [gr-qc]
59. S.H. Hendi, M. Momennia, Reentrant phase transition of Born–Infeld–dilaton black holes. *Eur. Phys. J. C* **78**(10), 800 (2018). <https://doi.org/10.1140/epjcs10052-018-6278-y> [arXiv:1709.09039 [gr-qc]]
60. B.R. Majhi, S. Samanta, P–V criticality of AdS black holes in a general framework. *Phys. Lett. B* **773**, 203 (2017). <https://doi.org/10.1016/j.physletb.2017.08.038> [arXiv:1609.06224 [gr-qc]]
61. K. Bhattacharya, B.R. Majhi, Thermogeometric description of the van der Waals like phase transition in AdS black holes, *Phys. Rev. D* **95**(10), 104024 (2017). <https://doi.org/10.1103/PhysRevD.95.104024> [arXiv:1702.07174 [gr-qc]]
62. K. Bhattacharya, B.R. Majhi, S. Samanta, Van der Waals criticality in AdS black holes: a phenomenological study. *Phys. Rev. D* **96**(8), 084037 (2017). <https://doi.org/10.1103/PhysRevD.96.084037> [arXiv:1709.02650 [gr-qc]]
63. P. Wang, H. Wu, H. Yang, Thermodynamics and phase transition of a nonlinear electrodynamics black hole in a cavity, arXiv:1901.06216 [gr-qc]
64. B.P. Dolan, Pressure and volume in the first law of black hole thermodynamics. *Class. Quantum Gravity* **28**, 235017 (2011). <https://doi.org/10.1088/0264-9381/28/23/235017> [arXiv:1106.6260 [gr-qc]]
65. R. Penrose, Gravitational collapse and space-time singularities. *Phys. Rev. Lett.* **14**, 57 (1965). <https://doi.org/10.1103/PhysRevLett.14.57>